Effect of well coupling on the TE optical modal gain in quantum-well-based semiconductor lasers

2002 J. Phys.: Condens. Matter 14 L83

(http://iopscience.iop.org/0953-8984/14/4/102)

INSTITUTE OF PHYSICS PUBLISHING JOURNAL OF PHYSICS: CONDENSED MATTER

J. Phys.: Condens. Matter **14** (2002) L83–L87 PII: S0953-8984(02)31195-0

LETTER TO THE EDITOR

Effect of well coupling on the TE optical modal gain in quantum-well-based semiconductor lasers

P Weetman[1], **M Kucharczyk and M S Wartak**[1]

Department of Physics and Computing, Wilfrid Laurier University, Waterloo, Ontario, Canada N2L 3C5
and
LASMA INC, 306 Faraday Court, Waterloo, Ontario, Canada N2L 6A6

Received 23 November 2001
Published 18 January 2002
Online at stacks.iop.org/JPhysCM/14/L83

Abstract

The role of coupling between two quantum wells in TE optical modal gain is analysed within the self-consistent solution of the Poisson, Schrödinger and 4×4 Luttinger–Kohn equations. The many-body effects of bandgap renormalization, coulombic scattering interactions and a non-Markovian distribution are also included. The analysis is performed for a 1.55 μm InGaAsP/InP lattice-matched system grown in the [001] direction. It shows that electrostatics significantly changes the modal gain in both amplitude and spectrum. The gain amplitude is larger when electrostatic effects are included due to better charge localization in the wells. The gain spectrum also changes due to the modification of the heterostructure potential and hence different coupling between the wells.

Semiconductor lasers based on quantum wells (QWs) are playing an important role in today's optoelectronic applications. Their properties are constantly improved. Many of those improvements are linked to fundamental physical properties of those devices (see e.g. [1]). One of the physical parameters which significantly affect operation of QW-based devices is coupling between wells. For a double-quantum-well (DQW) system, when the separation barrier is thin enough, coupling between the two wells becomes important [2, 3]. The effect of well coupling on the optical modal gain of multi-QW lasers has been studied by Akhtar *et al* [2], and Sarmento [4] using the parabolic band model. It is known [5], however, that in QWs the gain peak determined with the band-mixing effects included is significantly reduced (1.5–2-fold) when compared with the conventional parabolic band model.

Electrostatic self-consistency has also the well known effect of altering the potential profile and the distribution of carriers in QW heterostructures [6, 7]. Studies on the consequences of this on the optical gain of single-quantum-well (SQW) lasers have been performed [7]. The effects noted are mainly due to the change in charge distribution (although it must be kept in

[1] Work partially performed while the authors were at VTT Electronics, Kaitovayla 1, PO Box 1100, FIN-90571, Oulu, Finland.

mind that Seki *et al* [7] also incorporated a change in the dephasing time which we will not do in order to examine only electrostatic effects). Since electrostatic self-consistency changes the potential profile, there will also be a change in the well coupling effects.

In this Letter we report on the study of well coupling effects and electrostatic effects on the TE modal gain in a DQW laser. This will be done by calculating the TE modal gain versus frequency at various barrier separation widths with and without electrostatic self-consistency. We describe the various calculations and methods required to arrive at a final gain expression incorporating these effects.

In order to calculate the electrostatic effect on the heterostructure potential energy, we must solve for the conduction and valence wavefunctions self-consistently with Poisson's equation (in this paper, the structure is undoped) [6, 8, 9].

$$\frac{\mathrm{d}}{\mathrm{d}z}\left[\varepsilon(z)\frac{\mathrm{d}}{\mathrm{d}z}\phi(z)\right] = -e(\rho_{\mathrm{HH}}(z) + \rho_{\mathrm{LH}}(z) - \rho_{\mathrm{c}}(z)) \tag{1}$$

where e is the fundamental charge, $\varepsilon(z)$ is the position-dependent permittivity, $n(z)$, $p(z)$ are the position-dependent electron and hole band density distributions respectively. The function $\phi(z)$is the electrostatic potential.

These density distributions are [6]

$$\rho_\alpha(z) = \frac{k_{\mathrm{B}}T}{\pi\hbar^2}\left(\sum_n \bar{m}^*_\alpha \left|F^\alpha_n(z)\right|^2 \ln\left[1 + \exp\left(\frac{E^{\mathrm{f}}_\alpha - E^\alpha_n}{k_{\mathrm{B}}T}\right)\right]\right). \tag{2}$$

The symbol α represents the conduction (c), heavy-hole (HH) and light-hole (LH) bands and n is an index over the subbands. $E^{\mathrm{f}}_{\mathrm{c}}$ is the conduction band Fermi-level and $E^{\mathrm{f}}_{\mathrm{HH}} = E^{\mathrm{f}}_{\mathrm{LH}}$ is the valence band Fermi-level. These are determined by standard methods [1]. The symbol k_{B} is Boltzmann's constant, T is temperature, $\bar{m}^*_\alpha$ is the average effective mass for the particular band, which will be taken as approximately the effective mass in the wells since most of the carriers are confined there. $F^\alpha_n(z)$ and E^α_n are the respective envelope eigenfunctions and eigenvalues of the various subbands in the parabolic approximation at the band-edge.

Having expressions for the wavefunctions and electrostatic potential, self-consistency iteration such as Stern's 'fixed convergence factor' method [6, 9] is then used to calculate the change in the heterostructure potential.

For calculating optical gain, the conduction band envelope functions are once again determined using the parabolic effective mass equation. The valence band envelope functions, however, are now determined by using a more accurate model based on the 4×4 Luttinger–Kohn (LK) Hamiltonian [1, 3]. The reason for using two approximations for the valence band is that the parabolic method is significantly faster, but only gives accurate results near the band-edge for the first few subbands. This turns out to be sufficient to calculate the electrostatic effects, but not for the overlap integrals required in the gain calculations.

Our gain calculations incorporate bandgap renormalization, coulombic and non-Markovian effects [7, 10–14]. To incorporate bandgap renormalization, we use the phenomenological approximation $\Delta E \simeq \beta N^{1/3}$. Here N is the average carrier density in the wells (electrons or holes) and β is a bandgap renormalization coefficient chosen to equal the shift found by a more detailed calculation [10, 12] at a specific concentration.

The coulombic and non-Markovian effects are incorporated by using the gain equation [14]

$$g(E) = \frac{E\mu c}{\hbar n_r V}\sum_{\sigma\eta lm}\sum_{\boldsymbol{k}_\parallel} |\hat{\varepsilon}\cdot \boldsymbol{M}^{\eta\sigma}_{lm}(\boldsymbol{k}_\parallel)|^2 \frac{(f^l_c - f^m_{h\sigma})\mathrm{Re}\ \Xi^{\eta\sigma}_{lm}(0, \Delta^{\eta\sigma}_{lm}(\boldsymbol{k}_\parallel))[1+\mathrm{Re}\ g_2(\infty, \Delta^{\eta\sigma}_{lm}(\boldsymbol{k}_\parallel))]}{1 - \mathrm{Re}\, q^{\eta\sigma}_{1_{lm}}(\boldsymbol{k}_\parallel)} \tag{3}$$

where $E = \hbar\omega$ is the photon energy. The details of this equation can be found in [14].

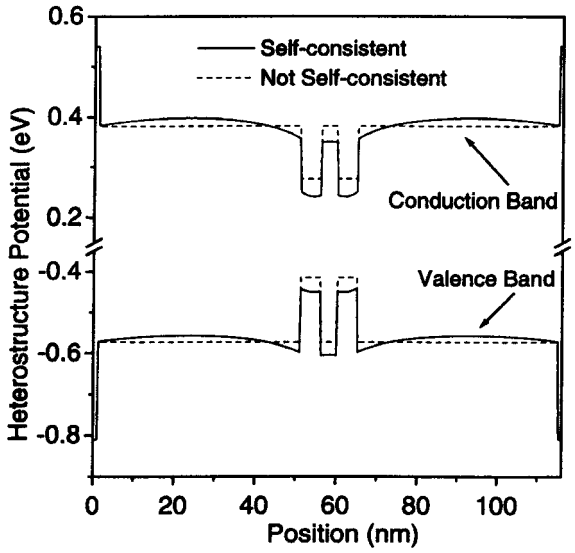

Figure 1. The heterostructure potential versus position for a separation barrier width of 4 nm and an average well carrier density 4.5×10^{18} cm^{-3}.

The structure simulated consists of two 5 nm QWs with a varying separation barrier and 500 nm fixed barriers on either side. All barriers are InGaAsP with bandgap 1.1 μm. The cladding and substrate surrounding the structure are InP. The wells and barriers are InGaAsP and lattice matched to InP so there is no strain in the system. The composition of the wells is chosen such that maximum gain occurs around 1.55 μm (this is an approximate relation because the energy at maximum gain will change depending on carrier density and separation barrier width, see figure 3). All layers are assumed to be grown in the [001] direction. Standard material parameters and bandgap calculations were used [15].

The wavefunctions in the parabolic approximation and Poisson's equation were solved numerically using a finite difference method. For the LK Hamiltonian approximation, a plane wave expansion method was used [3]. We experimented with using the parabolic and LK approximations for the valence band to calculate the electrostatic effects. Very little difference was found between them with respect to the modification to the heterostructure. The parabolic approximation, however, was of the order of one hundred times faster than the LK approximation in terms of CPU time.

Figure 1 shows how self-consistency modifies the original heterostructure potential. Inclusion of electrostatic effects modifies the system so as to move it closer to local charge electroneutrality [7]. This modification causes more conduction electrons and fewer holes to be confined within the wells (figure 2). Since conduction electrons are normally the limiting factor to gain, the higher confinement of electrons in the wells results in larger gain amplitude (figures 3, 4). Electrostatic effects also cause the gain spectrum to change. As noted by others [2, 3] varying separation barrier widths will change the relative strength of each subband transition. Self-consistency modifies the potential profile and consequently the relative transition strengths. Therefore the gain spectrum will depend on the well separation and the electrostatics as demonstrated in figure 3. In figure 4 the maximum gain is significantly larger for the electrostatic case for most barrier widths. As well, the barrier separation for minimum gain is smaller when electrostatics is included. This can be explained by figure 3,

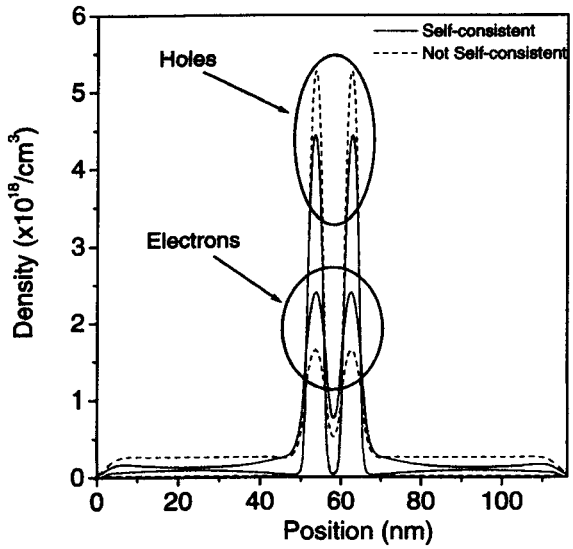

Figure 2. The density distribution of electrons and holes versus position for a separation barrier width of 4 nm and an average well carrier density 4.5×10^{18} cm^{-3}.

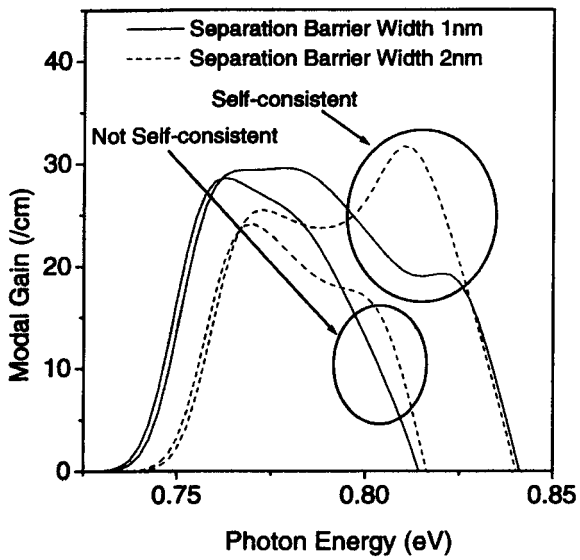

Figure 3. The TE modal gain versus photon energy for an average well carrier density 4.5×10^{18} cm^{-3}.

where we see that the dominant transition has changed already between the 1.0 and 2.0 nm barriers when electrostatics is included, but it has not yet if electrostatics is not included.

In conclusion, we have found that electrostatic effects can significantly modify the potential profile of the DQW laser. This causes changes in the gain in two ways. First, it increases the conduction electron density and reduces the hole density in the active region, which increases the gain amplitude. Second, the spectral properties will be modified since a change in the profile changes the relative strength of each subband transition. These effects have a

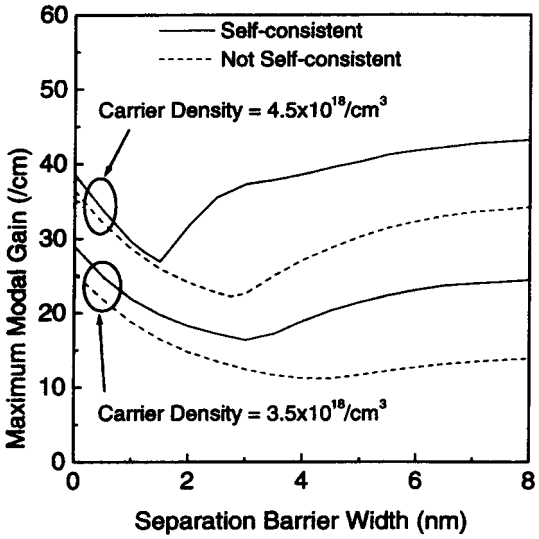

Figure 4. The maximum modal gain versus separation barrier width for two different carrier densities.

large practical importance. The energy at maximum gain is altered, which is an important consideration in the design of an efficient laser. Also, we can determine the minimum separation barrier width above which the gain will remain relatively uniform. An accurate model for a DQW laser should therefore take electrostatics into account. During the course of the calculations, it was also found that it is not necessary to have a rigorous model for the valence bands to determine the electrostatic modifications of the heterostructure. A parabolic approximation for all bands is sufficient and saves considerable computation time.

We would like to acknowledge the support from the Natural Science and Engineering Research Council of Canada (NSERC), Photonics Research Ontario (PRO), Canadian Institute for Photonic Innovations (CIPI), Industrial Research Assistance Program (IRAP) and VTT Electronics, Oulu, Finland. We would also like to thank Richard Voino and Daniel Nedelko of Wilfrid Laurier University for their much needed and appreciated computer assistance.

References

[1] Chuang S L 1995 *Physics of Optoelectronics Devices* (New York: Wiley)
[2] Akhtar A I, Guo C-Z and Xu J M 1993 *J. Appl. Phys.* **73** 4579
[3] Kucharczyk M, Wartak M S and Rusek P 1999 *Microw. Opt. Technol. Lett.* **22** 301
[4] Sarmento A D 1995 *Proc. SPIE* **2610** 23
[5] Chen P A, Chen C Y and Juang C 1994 *J. Appl. Phys.* **76** 85
[6] Chen P A, Juang C and Chang C Y 1993 *IEEE J. Quantum Electron.* **29** 2607
[7] Seki S, Yokoyama K and Sotirelis P 1995 *IEEE J. Select. Top. Quantum Electron.* **1** 264
[8] Tan I H, Snider G L, Chang L D and Hu E L 1990 *J. Appl. Phys.* **68** 4071
[9] Stern F and Das Sarma S 1970 *J. Comput. Phys.* **6** 56
[10] Hsu C H, Zory P S, Wu C and Emanuel M A 1997 *IEEE J. Select. Top. Quantum Electron.* **3** 158
[11] Connely M J 2001 *IEEE J. Quantum Electron.* **37** 439
[12] Chow W W, Koch S W and Sargent M III 1997 *Semiconductor-Laser Physics* (Berlin: Springer)
[13] Minch J, Park S H, Keating T and Chuang S L 1999 *IEEE J. Quantum Electron.* **35** 771
[14] Ahn D 1996 *IEEE J. Quantum Electron.* **32** 960
[15] Ishikawa T and Bowers J E 1994 *IEEE J. Quantum Electron.* **30** 563